

Research



Cite this article: Zossi BS, Medina FD, Tan Jun G, Lastovicka J, Duran T, Fagre M, de Haro Barbas BF, Elias AG. 2023 Extending the analysis on the best solar activity proxy for long-term ionospheric investigations. *Proc. R. Soc. A* **479**: 20230225.
<https://doi.org/10.1098/rspa.2023.0225>

Received: 1 April 2023

Accepted: 11 July 2023

Subject Areas:

atmospheric science, geophysics

Keywords:

solar activity proxy, foF2 modelling, ionosphere, long-term trends

Author for correspondence:

Ana G. Elias

e-mail: aelias@herrera.unt.edu.ar

Extending the analysis on the best solar activity proxy for long-term ionospheric investigations

Bruno S. Zossi^{1,2}, Franco D. Medina^{1,2}, Gloria Tan Jun³, Jan Lastovicka⁴, Trinidad Duran^{5,6}, Mariano Fagre^{7,8}, Blas F. de Haro Barbas^{1,2} and Ana G. Elias^{1,2}

¹Laboratorio de Ionosfera, Atmosfera Neutra y Magnetosfera (LIANM), FACET, Universidad Nacional de Tucumán (UNT), Argentina

²INFINOA, CONICET-UNT, Argentina

³German Aerospace Center (DLR), Institute for Solar-Terrestrial Physics, Neustrelitz, Germany

⁴Institute of Atmospheric Physics, Czech Academy of Sciences, Prague, Czech Republic

⁵Departamento de Física, Universidad Nacional del Sur (UNS), Bahía Blanca, Argentina

⁶Instituto de Física del Sur (CONICET-UNS), Bahía Blanca, Argentina

⁷Consejo Nacional de Investigaciones Científicas y Técnicas, CONICET, Argentina

⁸Laboratorio de Telecomunicaciones (LABTEL), FACET, UNT, Argentina

BSZ, 0000-0002-4197-7876; JL, 0000-0002-1454-3183; MF, 0000-0002-0073-6371; AGE, 0000-0001-6271-4891

Based on a previous study to select the best solar activity proxy for foF2 modelling, we expand the analysis to include 24 h time span, increase the spatial coverage by considering additional ionospheric stations, and update the analysis to 2021. Annual means of foF2 are analysed for 12 selected stations from Europe, Asia and Oceania, with high-quality data covering the period 1978–2021 in most of the cases, including two of the three European stations of the previous study. The same four solar proxies were used: F10.7, F30, MgII and HeII, which, based on the high linear correlation between each of them and foF2, serve to model this ionospheric parameter

through a linear regression. The results of our comparative analysis, extended to more stations, all the hours and updated time series, agree with previous works, with MgII and F30 being the best solar proxies for foF2 modelling, while HeII is found to be the least effective for this purpose. The importance of the solar proxy selection to model foF2 for filtering purposes to later estimate long-term trends is highlighted considering that different solar proxies applied might result in somewhat different foF2 long-term trend values.

1. Introduction

The study of trends in the Earth's atmosphere is of great importance for its contribution to climate change research and its consequences [1]. The upper atmosphere, and in particular the ionosphere, also experiences long-term variations that, in order to be detected, require a filtering process. This, in turn, involves solar activity proxies of solar extreme ultraviolet (EUV) radiation variability. With the objective of finding the best solar proxies for long-term assessments of two ionospheric parameters (the critical frequencies of the F2 and E ionospheric layers, foF2 and foE, respectively), Lastovicka [2] analysed the performance of four solar EUV proxies: F10.7, F30, MgII and HeII. In addition to these four proxies, Lastovicka [3,4] considered Lyman α and the sunspot number. They are used to model these ionospheric parameters from European stations with long and homogeneous data series. He considered three stations in the case of foF2: Juliusruh (54.6° N, 13.4° W), Pruhonice (49.9° N, 14.6° E) and Rome (41.8° N, 12.5° E), and two in the case of foE: Juliusruh and Slough/Chilton (51.5° N, 1.3° W). The analysed period for foF2, 1976–2014, was divided into two sub-periods, 1976–1995 and 1996–2014, to take into account that the dependence of foF2 on solar proxies differs between these sub-periods for the selected stations [4]. The period 1976–1999 was considered for foE since data for later years (2000–2014) had quality problems [4,5].

The present study aims to extend the analysis made by Lastovicka [2] for foF2, expanding the time coverage from noontime values to encompassing data from all hours of the day, increasing the spatial coverage and updating the data period to 2021.

2. Data

Monthly median foF2 data used in this work was acquired from free access repositories. The location of 12 selected stations and their analysed period are listed in table 1. Years with more than 50% missing data were removed. In all the cases, the initial year is 1978, the starting year of the solar EUV proxy with the latest start, which is the MgII index. Its record starts in November 1978 [6].

The Japanese stations' foF2 data were obtained from https://wdc.nict.go.jp/IONO/index_E.html; Australian and European stations from <https://downloads.sws.bom.gov.au/wdc/iondata/au/> and the Damboldt and Suessman database [7] from <https://downloads.sws.bom.gov.au/wdc/iondata/medians/> and <https://downloads.sws.bom.gov.au/wdc/iondata/medians/foF2/>. Sodankyla was updated with data from https://www.sgo.fi/pub_ion/allmedians/, and Juliusruh from https://www.ionosonde.iap-kborn.de/mon_fof2.htm. In the case of Rome, the period was updated with data from Lowell GIRO Data Center (LGDC) [8].

The EUV solar proxies used are those considered by Lastovicka [2]: 10.7 cm solar flux (F10.7), 30 cm solar flux (F30), Mg II core-to-wing ratio (MgII), and He II 30.38 nm line (HeII). F10.7 is available from Space Weather Canada at <https://spaceweather.gc.ca/forecast- prevision/solar-solaire/solarflux/sx-en.php>; F30 and HeII are available at Laboratory for Atmospheric and Space Physics (LASP) Interactive Solar Irradiance Data Center at <https://lasp.colorado.edu/lisird>; MgII index is available from the University of Bremen at <http://www.iup.uni-bremen.de/UVSAT/datasets/mgii>.

Table 1. List of ionospheric stations used in this study, geographical location and range of years considered. Periods between brackets indicate missing or removed years.

station	latitude	longitude	years analysed
Wakkanai	45.2	141.8	1978–2021
Kokubunji	35.7	139.5	1978–2021
Yamagawa	31.2	130.6	1978–2019 (1988–2002)
Okinawa	26.7	128.2	1978–2021
Hobart	−42.5	147.2	1978–2021
Canberra	−35.2	149.2	1978–2021
Brisbane	−27.3	153.0	1978–2021 (1988–1997)
Townsville	−19.2	146.5	1978–2021
Sodankyla	67.3	26.3	1978–2021
Juliusruh	54.6	13.4	1978–2021
Rome	41.8	12.5	1978–2021
Uppsala	59.8	17.6	1978–2000

Monthly median foF2 time series were averaged over 3 h intervals centered at 0, 3, 6, 9, 12, 15, 18 and 21 LT. Annual means for each of these eight series for each station were estimated, and for each EUV solar proxy as well.

3. Methodology

The evaluation of the best solar proxy for foF2 modelling is carried out by comparing the modelled values using each proxy with foF2 observations (measured data). When comparing data to a model prediction, in general, more than one statistical index should be used. For example, the correlation coefficient, r , which measures the similarity in their time variation, or equivalently the squared correlation coefficient, r^2 , which measures the explained variance, together with any error measure (absolute error, mean bias, relative error and/or root mean square error), which quantifies the similarity in their values [9,10]. In our case, the modeled value is obtained from a least square method applied to the data itself, given by

$$\text{foF2} = A + B \times \text{solar EUV proxy}, \quad (3.1)$$

where foF2 is deseasonalized. This can be done considering, for example, 12-month running means or annual time series of foF2 and solar EUV proxies. This is also the approach used to filter solar activity effects from foF2 previous to its long-term trend estimation. In this kind of modelling (resulting from a least square fit) r or r^2 , and the error measures based on squared formulae give the same information. While the mean error obtained simply as the average of the difference between the experimental data and the model prediction is zero, that is it does not give any additional information. Our analysis will be based then, as in Lastovicka [2], in r^2 which gives the foF2 percentage variance, explained by each of the four EUV solar proxies according to equation (3.1).

Lastovicka [2] divided the analysed period into two sub-periods: before and after 1996. This was done to take into account that the dependence of foF2 on solar proxies differs between these sub-periods, as was observed for the three selected stations in Lastovicka's work [4]: Juliusruh, Pruhonice, and Rome. He noticed that in the linear regression model often used to remove the solar cycle effect from this ionospheric parameter, given by equation (3.1), the coefficient B is not stable along the whole data period. He proved this by analysing the time evolution of this

coefficient calculated with a sliding 11-year window along the whole analysed period that was 1976–2014 [4]. A step increase in B values was observed around 1996 so that along period 1976–1995, B values were, in general, lower than along 1996–2014 indicating that the dependence of foF2 on solar activity proxies is stronger in the latter period.

In this work, we perform first the analysis of B stability using the 11-year running window in order to determine the need, or not, of splitting the analysed period, followed by the r^2 analysis of each solar EUV proxy to determine its performance in foF2 modelling. The effect of the choice of this proxy on the value of the trend is then shown as a consequence of choosing one or another proxy to model foF2.

4. Results

To begin, we performed B-stability analysis on 10 of the 12 stations here analysed. Yamagawa and Brisbane were withdrawn in the case of this particular analysis due to the missing data (table 1). Figure 1 shows the evolution of B-coefficient using an 11-year moving window and F10.7 as EUV solar proxy. The approximately 1996 step observed in Juliusruh, Rome, and Pruhonice by Lastovicka [4] is not evinced by the other stations in this work. The Japanese and Australian stations, together with Sodankyla, present a step increase near the deep solar minimum of 2008.

Lastovicka [4] pointed out two possible reasons for the step increase in B observed around 1996: changes in the relation between the proxies and solar radiation, and changes between the ionospheric parameters and the solar radiation. In this work, several more stations were studied and the period of analysis increased in almost a decade. Even though the approximately 1996 step increase in B value is still observed, it is less noticeable. However, as in Lastovicka [4], a common behaviour is noticed that is a general increasing rate along the period in most of the stations. The new feature observed in this case is a step increase in some stations around 2008.

The same positive trend detected here in B coefficient for stations located in different hemispheres and magnetic latitudes (figure 1) could point toward a physical process with a stationary trend along the analysed period. For example, the Gleissberg cycle [11], one of the longest known solar periodicities, is in its declining phase since approximately 1985. This long-term periodicity is also present in geomagnetic activity and, even though it is weak, it may play a role. Another possible mechanism is the magnetic field dipolar decrease over the last century. However, as mentioned in Lastovicka [4], the ionospheric processes are very complex. They involve not only ionizing radiation from the sun and non-uniform spatial and temporal effects of geomagnetic activity but also transport processes that play a significant role in the F2 layer. Therefore, a comprehensive and detailed analysis is essential before reaching a definitive conclusion. Considering that there is not a well-defined step variation in a common year for all the stations analysed, a linear regression to the complete period was considered instead of separate sub-periods as in Lastovicka [2].

Turning now to the evaluation of the best solar proxy for foF2 modelling, we estimated r^2 for each station and at each 3-hour interval considering the four different solar proxies. Figure 2 shows r^2 diurnal variation for each case evincing that MgII (green dots) and F30 (orange dots) are generally the EUV solar proxies that best correlate with foF2 along all hour bins and stations. HeII (red dots) has the lowest r^2 values, in agreement with the results of Lastovicka [2].

Another way of looking at the differences in each EUV solar proxy performance is through a histogram. Figure 3 shows r^2 distribution considering annual values, for all eight 3-hour bin time series. The solar proxies with the greatest frequency at the highest r^2 value are MgII and F30, with HeII presenting the lowest frequency at higher values.

A noticeable consequence of choosing a given solar EUV proxy to model foF2 should be detected in studies focusing on the remaining foF2 variance after removing that linked to solar activity variation. This remaining variance amounts at most to approximately 10%, and it is the case of the long-term trend in ionospheric parameters expected from greenhouse gases concentration increase as a main driver, or from the secular variation of the Earth's magnetic field [12]. Figure 4 shows, as an example, foF2 residuals after filtering the variability linked to

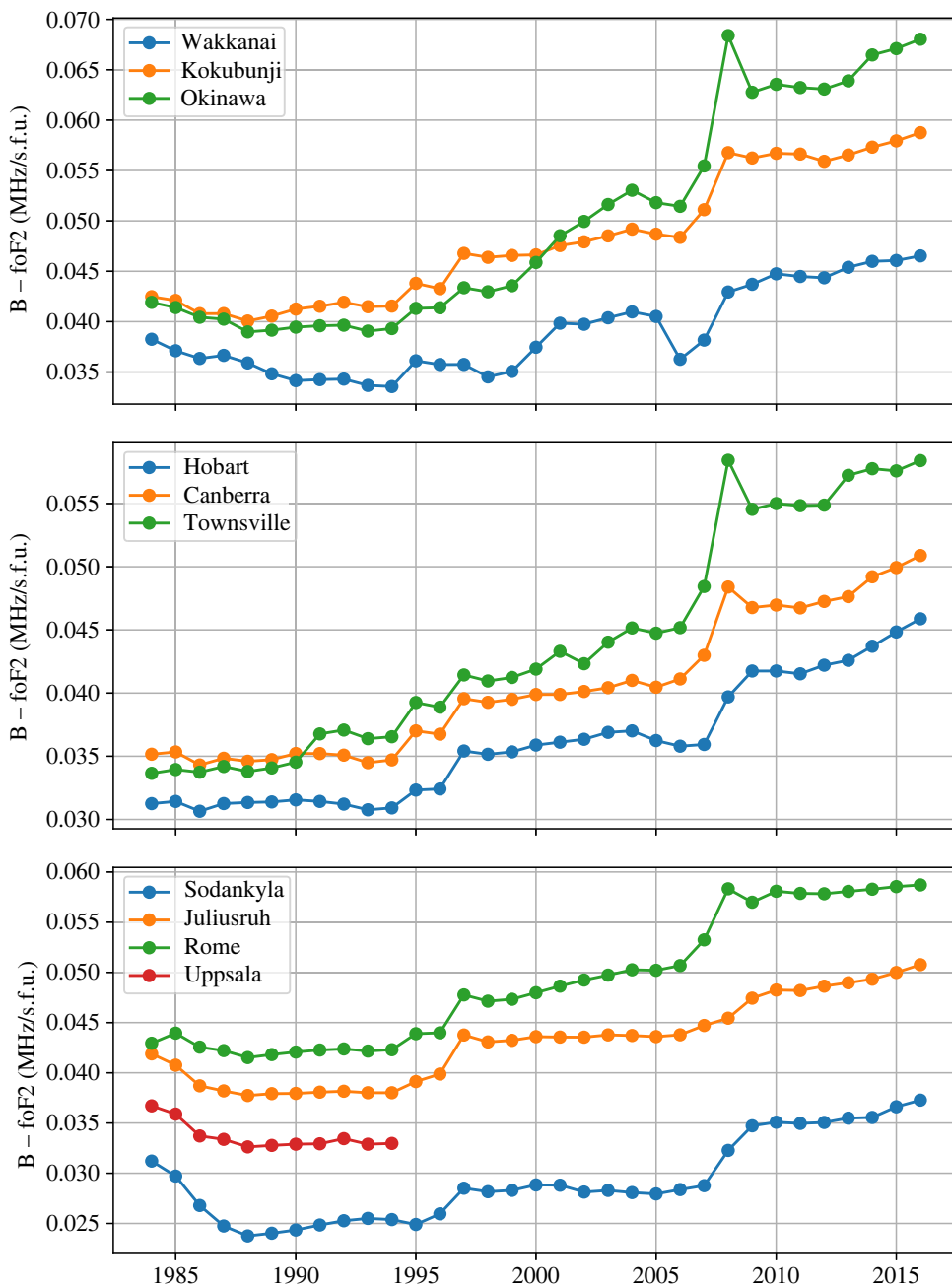


Figure 1. Coefficient B from the linear regression between foF2 and F10.7 using an 11-year moving window, for Japanese (upper panel), Australian (middle panel) and European (lower panel) stations, for foF2 11–12–13 LT average.

solar activity through equation (3.1), for two of the 3-hour bins: one centered at 0 LT (nighttime) and other centered at 12 LT (noon) for a Japanese, an Australian and a European station. Figure 5 presents trend values for these selected stations for each 3-hour bin showing clearly that different trend values, and even with different signs, are obtained depending on the solar EUV proxy selected in the step previous to trend calculation. foF2 trends obtained after filtering solar activity using MgII, F30 and F10.7 present slightly different values but with a similar diurnal variation. In the case of HeII, which is the one with the lowest r^2 in general, as can be noticed

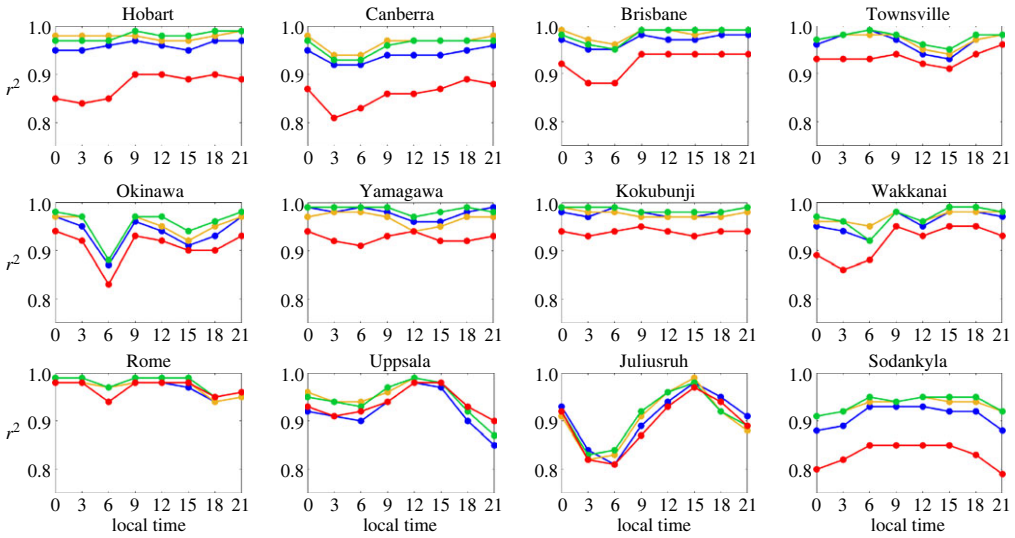


Figure 2. Squared correlation coefficient, r^2 , between foF2 annual mean and EUV solar proxies: F10.7 (blue), F30 (orange), MgII (green) and Hell (red). The local time value in the abscissa indicates the centre of the averaged 3-hour interval.

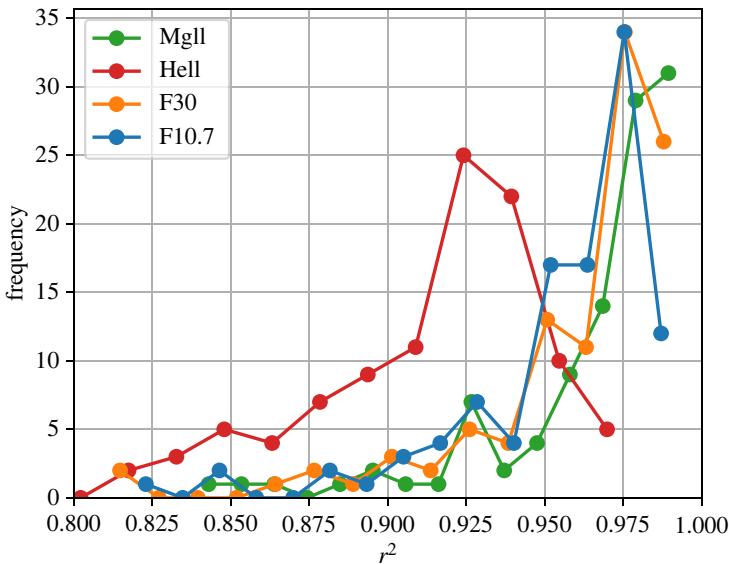


Figure 3. Histogram of r^2 between foF2 and EUV solar proxies: F10.7 (blue), F30 (orange), MgII (green) and Hell (red) considering annual values and all the 3 h ranges.

in figure 2, yield the greatest differences, not only in trend values, but also in their diurnal variation.

5. Conclusion

Lastovicka [2] studied foF2 from three European stations: Juliusruh (54.6° N, 13.4° W), Pruhonice (49.9° N, 14.5° E), and Rome (41.8° N, 12.5° E) considering noontime values. In the present work, we extended the area of study in order to generalize his results using stations in the

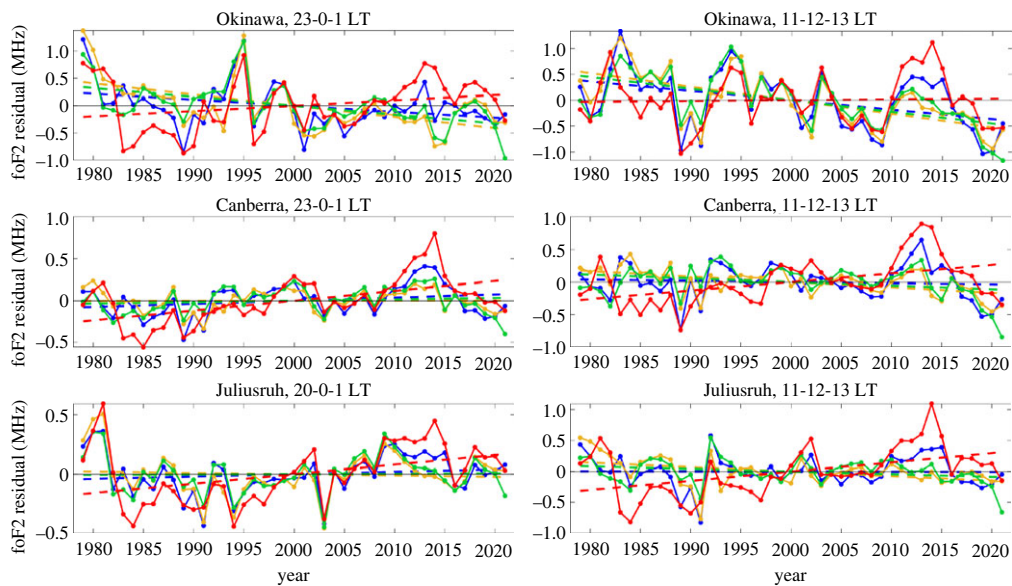


Figure 4. foF2 residuals (MHz) from the linear regression in equation (3.1), considering as solar EUV proxies: F10.7 (blue), F30 (orange), MgII (green) and HeII (red), for a Japanese (Okinawa), an Australian (Canberra) and a European (Juliusruh) station, together with the corresponding linear trends (dashed lines), for night-time (23–0–1 LT mean) and noontime (11–12–13 LT mean).

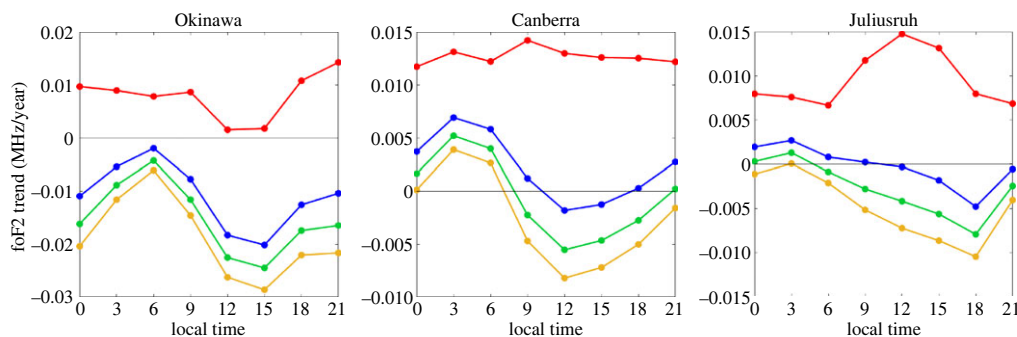


Figure 5. Diurnal variation of foF2 trends (MHz/year) using the linear regression in equation (3.1) to filter solar activity variation, considering as solar EUV proxies: F10.7 (blue), F30 (orange), MgII (green) and HeII (red), for a Japanese (Okinawa), an Australian (Canberra) and a European (Juliusruh) station.

northern and southern hemispheres and all local times. In addition, the time series were updated to 2021.

The analysis of B regression coefficient was extended for 10 ionospheric stations and, as can be noticed in figure 1, all of them exhibit an increasing trend. This means, on average, that the ionospheric electron density, calculated using foF2, increases more rapidly with the solar activity in present times. The causes of these changes, as well as the distinctive steps observed at different years using the applied method, require more investigation.

The squared correlation coefficient analysis, presented in figure 2, for each station at different local times, shows the lead of MgII and F30 proxy to reproduce foF2. There are some cases when MgII outperforms F30, and others where F30 performs the best. HeII is clearly the least adequate proxy in all the cases.

More recently, Danilov & Konstantinova [13] and Danilov & Berbeneva [14] analysed also the adequacy of EUV solar proxies for foF2 trend estimation considering Juliusruh data along the period 1996–2022 for different local times, as in this work, but adding a seasonal analysis. Even though they focus their study in the trend analysis, they recommend not only MgII and F30 as the best proxies in foF2 for trend estimation, but also Lyman α flux, which is not included in the present analysis. Lastovicka & Buresova [15] analysed noon annual mean foF2 from several stations covering mid and low latitudes along the period 1976–2014, and also include Lyman α flux as an additional proxy. They again find MgII and F30 as the best solar proxies for foF2 variability, but for mid-latitude stations. In the case of equatorial stations, where they include Okinawa and Townsville, they point out HeII as the best proxy. However, they mention these two stations, located rather in the transitional zone between dominance of MgII and F30 versus HeII, with rather marginal differences between their roles. So, our results would be in agreement with this more recent analysis made by Lastovicka & Buresova [15]. These three latest studies set a clear path for us to continue, conducting a seasonal analysis, adding ionospheric stations to cover a wider latitudinal range, and further exploring the effect on the foF2 trend values.

Going back to our results, one could argue that what remains unexplained after modelling foF2 with any of the proxies used in this study is on the order of 10% or even less. But precisely, this is the order of the variance linked to long-term trends in the ionosphere associated mainly with the greenhouse gases increasing concentration effect during the last decades. Thus, trends should be sensitive to the solar EUV proxy used in the filtering process previous to trend assessment. This is shown in figures 4 and 5 which present as an example the trends for three out of the 12 stations here analysed. With MgII and F30 being the solar EUV proxies with the highest r^2 values, they are the ones recommended for foF2 long-term trend estimations, followed by F10.7.

Data accessibility. All ionospheric and indexes data are freely available in the following repositories: the Japanese stations' data from https://wdc.nict.go.jp/IONO/index_E.html; Australian and European stations from <https://downloads.sws.bom.gov.au/wdc/iondata/au/> and the Damboldt and Suessman database at <https://downloads.sws.bom.gov.au/wdc/iondata/medians/> and <https://downloads.sws.bom.gov.au/wdc/iondata/medians/foF2/>. Sodankylä was updated from https://www.sgo.fi/pub_ion/allmedians/, Juliusruh from https://www.ionosonde.iap-kborn.de/mon_fof2.htm, and Rome from <http://spase.info/SMWG/Observatory/GIRO>. F10.7 is available from Space Weather Canada at <https://spaceweather.gc.ca/forecast- prevision/solar-solaire/solarflux/sx-en.php>; F30 and HeII are available at LASP Interactive Solar Irradiance Data Center <https://lasp.colorado.edu/lisird>; MgII index is available from the University of Bremen at <http://www.iup.uni-bremen.de/UVSAT/datasets/mgii>.

Authors' Contributions. B.S.Z.: conceptualization, formal analysis, investigation, methodology, writing—original draft; F.D.M.: investigation, methodology, writing—review and editing; G.T.J.: investigation, methodology, writing—review and editing; J.L.: conceptualization, formal analysis, methodology, writing—review and editing; T.D.: methodology, writing—review and editing; M.F.: methodology, writing—review and editing; B.F.H.B.: formal analysis, methodology, writing—review and editing; A.G.E.: investigation, methodology, writing—review and editing.

All authors gave final approval for publication and agreed to be held accountable for the work performed therein.

Conflict of interest declaration. The authors declare that they have no conflict of interest.

Funding. J. Lastovicka acknowledges the Czech Science Foundation project no. 21-03295S. T. Duran acknowledge research project nos. PICT 2019-03491 and PGI 24/F083.

Acknowledgements. We acknowledge the Sodankylä Geophysical Observatory, the Leibniz Institute of Atmospheric Physics, GIRO data resources, the Australian Bureau of Meteorology, and the National Research and Development Agency - Information and Communications Technology, NICT, for providing ionospheric data. B.S. Zossi, F.D. Medina, B.F. de Haro Barbas and A.G. Elias acknowledge research project PIP 2957.

References

1. IPCC. 2022 Climate Change 2022: Impacts, Adaptation, and Vulnerability. In *Contribution of Working Group II to the Sixth Assessment Report of the Intergovernmental Panel on Climate Change*

- (eds H-O Pörtner *et al.*), 3056 pp. Cambridge, UK and New York, NY: Cambridge University Press. (doi:10.1017/9781009325844)
2. Lastovicka J. 2021 The best solar activity proxy for long-term ionospheric investigations. *Adv. Space Res.* **68**, 2354–2360. (doi:10.1016/j.asr.2021.06.032)
 3. Lastovicka, J., 2021 What is the optimum solar proxy for long-term ionospheric investigations? *Adv. Space Res.* **67**, 2–8. doi:10.1016/j.asr.2020.07.025
 4. Lastovicka J. 2019 Is the relation between ionospheric parameters and solar proxies stable? *Geophys. Res. Lett.* **46**, 14 208–14 213. (doi:10.1029/2019GL085033)
 5. Lastovicka J, Buresova D, Kouba D, Krizan P. 2016 Stability of solar correction for calculating ionospheric trends. *Ann. Geophys.* **34**, 1191–1196. (doi:10.5194/angeo-34-1191-2016)
 6. Viereck RA, Floyd LE, Crane PC, Woods TN, Knapp BG, Rottman G, Weber M, Puga LC, DeLand MT. 2004 A composite MgII index spanning from 1978 to 2003. *Space Weather* **2**, S10005. (doi:10.1029/2004SW000084)
 7. Damboldt T, Suessmann P. 2012 Consolidated Database of Worldwide Measured Monthly Medians of Ionospheric Characteristics foF2 and M(3000)F2. INAG (Ionosonde Network Advisory Group) Bulletin 73. See https://www.ursi.org/files/CommissionWebsites/INAG/web-73/2012/damboldt_consolidated_database.pdf.
 8. Reinisch BW, Galkin IA. 2011 Global ionospheric radio observatory (GIRO). *Earth Planets and Space* **63**, 377–381. (doi:10.5047/eps.2011.03.001)
 9. Willmott CJ, Matsuura K. 2005 Advantages of the mean absolute error (MAE) over the root mean square error (RMSE) in assessing average model performance. *Clim. Res.* **30**, 79–82. (doi:10.3354/cr030079)
 10. Chicco D, Warrens MJ, Jurman G. 2021 The coefficient of determination R-squared is more informative than SMAPE, MAE, MAPE, MSE and RMSE in regression analysis evaluation. *Peer J. Comput. Sci.* **7**, e623. (doi:10.7717/peerj-cs.623)
 11. Gleissberg W. 1943 Systematic fluctuations of the characteristics of sunspot cycles. *Observatory* **65**, 24–27.
 12. Lastovicka J. 2021 Long-Term Trends in the Upper Atmosphere. In *Upper atmosphere dynamics and energetics* (eds W Wang, Y Zhang, LJ Paxton), pp. 325–344. Washington, DC: American Geophysical Union.
 13. Danilov A, Konstantinova A. 2023 Trends in foF2 to 2022 and various solar activity indices. *Adv. Space Res.* **71**, 4594–4603. (doi:10.1016/j.asr.2023.01.028)
 14. Danilov AD, Berbeneva NA. 2023 Trends in the Critical Frequency of the F2 Layer during the Recent Decade. *Geomagn. Aeron.* **63**, 113–120. (doi:10.1134/S0016793222600886)
 15. Lastovicka J, Buresova D. 2023 Relationships between foF2 and various solar activity proxies. *Space Weather* **21**, e2022SW003359. (doi:10.1029/2022SW003359)